other two. Considering that radiation fog has the smallest particle-size distribution, our results should stand for this type of fog as well. Although we do not know the exact particle-size distribution of the fog in the measured link, the upslope fog is similar in formation to the advection fog; therefore, we also believe that, for this type of fog, the performance of the far-IR link should not be worse than those of the other two. Of course, present-day commercial technology still benefits shorter wavelengths, mostly due to the availability of low-cost sources and detectors. However, new technologies can produce competing devices for the far-IR window; thus our results demonstrate that it is worth working in the development of appropriate devices and systems because the optical channel indeed performs better at long wavelengths in most cases.

ACKNOWLEDGMENTS

This work was supported by the Research and Development Center of Ericsson Telecomunicações S/A, Brazil, and C. P. Colvero acknowledges scholarship support from the Brazilian Agency CNPq. The authors acknowledge the Brazilian state companies TVE Brasil and Furnas Centrais Elétricas S/A for allowing the installation of the transmitters and receivers within their facilities.

REFERENCES

1. A. Wastberg and B. Lundborg, Superposition of signals in ionospheric multipath channels, Radio Sci 32 (1997), 2083.
2. H. Weichel, Laser-beam propagation in the atmosphere, Bellingham, SPIE Optical Engineering TT3 (1990), 25–39.
3. S. Blaser, D. Hofstetter, M. Beck, and J. Faist, Free-space optical data link using Peltier-cooled quantum cascade laser, Electron Lett 37 (2001), 778–780.
4. R. Martini, R. Paiella, C. Gmachl, F. Capasso, E.A. Whittaker, H.C. Liu, H.Y. Hwang, D.L. Sivco, J.N. Baillargeon, and A.Y. Cho, High-speed digital data transmission using mid-infrared quantum cascade lasers, Electron Lett 37 (2001), 1290–1292.
5. R. Paiella, F. Capasso, C. Gmachl, C.G. Bethea, D.L. Sivco, J. Baillargeon, A.L. Hutchinson, A.Y. Cho, and H.C. Liu, Generation and detection of high-speed pulses of mid-infrared radiation with intersubband semiconductor lasers and detectors, IEEE Photon Technol Lett 12 (2000), 780–782.
6. R. Martini, C. Bethea, F. Capasso, C. Gmachl, R. Paiella, E.A. Whittaker, H.Y. Hwang, D.L. Sivco, J.N. Baillargeon, and A.Y. Cho, Free-space optical of multimedia satellite data streams using mid-infrared quantum cascade lasers, Electron Lett 38 (2002), 181–183.
7. F. Capasso, R. Paiella, R. Martini, R. Colombelli, C. Gmachl, T.L. Myers, M.S. Taubman, R.M. Williams, C.G. Bethea, K. Unterrainer, H.Y. Hwang, D.L. Sivco, A.Y. Cho, A.M. Sergent, H.C. Liu, and E.A. Whittaker, Quantum cascade lasers: Ultra-high speed operation, optical wireless communication, narrow linewidth, and far-infrared emission, IEEE J Quantum Electron (2002), 511–532.
8. A. Berk, L.S. Bernstein, G.P. Anderson, P.K. Acharya, D.C. Robertson, J.H. Chetwynd, and S.M. Adler-Golden, MODTRAN cloud and multiple scattering upgrades with application to AVIRIS, Remote Sens Environ 65 (1998), 367–375.
9. E. Korevaar, I. Kim, and B. McArthur, Debunking the recurring myth of a magic wavelength for free-space optics, Proc SPIE Opt Wireless Commun V, E.J. Korevaar (Editor), 4873 (2002), 155.
10. I. Kim, B. McArthur, and E. Korevaar, Comparison of laser beam propagation at 785 nm and 1550 nm fog and haze for optical wireless communications, Proc SPIE Opt Wireless Commun III 4214 (2001), 26–37.
11. H. Manor and S. Arnon, Performance of an optical wireless communication system as a function of wavelength, Appl Optics 42 (2003), 4285–4294.
12. M. Achour, Free-space optics wavelength selection: 10 μm versus shorter wavelengths, J Opt Netw 2 (2003), 127–143.
13. M. Achour, Simulating atmospheric free-space optical propagation: Rainfall attenuation, Proc SPIE 4635 (2002).
14. M. Achour, Simulating atmospheric free-space optical propagation: Part II, haze, fog and low clouds attenuations, Proc SPIE 4873 (2002).
15. A. Arnulf, J. Bricard, E. Curé, and C. Véret, Transmission by haze and fog in the spectral region 0.35 to 10 microns, J Opt Soc Amer 47 (1957), 491–498.
16. H. Koschmieder, Theorie der horizontalen sichtweite, Beitrage zur Physik der Freien Atmosphare 12 (1924), 33–53 (in German).

INTEGRATED INTERNAL GSM/DCS AND WLAN ANTENNAS WITH OPTIMIZED ISOLATION FOR A PDA PHONE

Kin-Lu Wong,[1] Jui-Hung Chou,[1] Chia-Lun Tang,[2] and Shih-Huang Yeh[2]

[1] Department of Electrical Engineering
National Sun Yat-Sen University
Kaohsiung 804, Taiwan
[2] Computer & Communications Research Laboratories
Industrial Technology Research Institute
Hsinchu 310, Taiwan

Received 1 February 2005

ABSTRACT: *Two internal antennas for GSM/DCS and WLAN operations printed and integrated on a dielectric substrate for application in a dual-network PDA phone are presented. The two integrated antennas are printed PIFAs mounted at the top edge of the main circuit board of the PDA phone, and the isolation behavior of the two antennas with various possible arrangements is studied. The optimized isolation between the two antennas is analyzed. Over the GSM, DCS, and WLAN bands, good isolation (less than −20 dB) between the two integrated antennas can be obtained.* © 2005 Wiley Periodicals, Inc. Microwave Opt Technol Lett 46: 323–326, 2005; Published online in Wiley InterScience (www.interscience.wiley.com). DOI 10.1002/mop.20977

Key words: *mobile antennas; GSM/DCS (global system for mobile communication/digital communication system) mobile antennas; WLAN (wireless local area network) antennas; PIFAs (planar inverted-F antennas); PDA (personal digital assistant) phones*

1. INTRODUCTION

Due to the recent successful deployment of wireless local area networks (WLANs) in numerous hotspots, it has become promising to integrate cellular and WLAN networks to provide ubiquitous or seamless data services for users [1, 2]. For this kind of integrated cellular/WLAN network application, it is expected that mobile phones or PDA phones capable of dual-network operation will become popular in the near future. For this promising application, many of the dual-network mobile or PDA phones are generally equipped with two antennas, one for cellular operation and another for WLAN operation. In this case, since there are limited spaces available inside the portable devices, isolation between the two antennas has become a critical issue. However, very little related information is available in the open literature.

Recently, a study on the isolation between two promising internal antennas—one GSM/DCS (890–960 MHz/1710–1880 MHz) antenna and one 2.4-GHz (2400–2484 MHz) WLAN antenna [3]—for a dual-network PDA phone has been presented [4]. The results have shown that with the GSM/DCS antenna fixed at the top edge of the system circuit board, optimized or near-optimized isolation is achieved when the WLAN antenna is placed

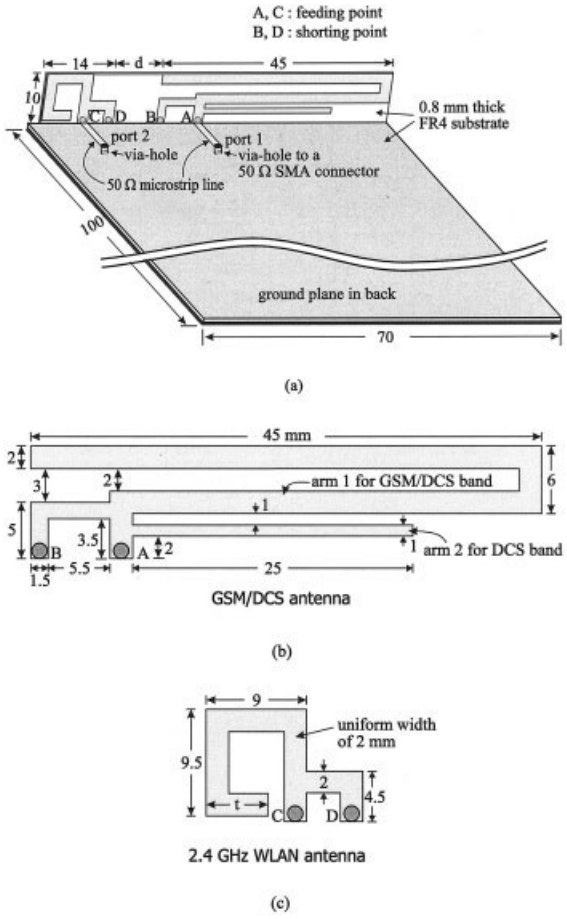

Figure 1 (a) Configuration of two integrated internal GSM/DCS and WLAN antennas for a dual-network PDA phone; dimensions of the (b) GSM/DCS and (c) WLAN antennas

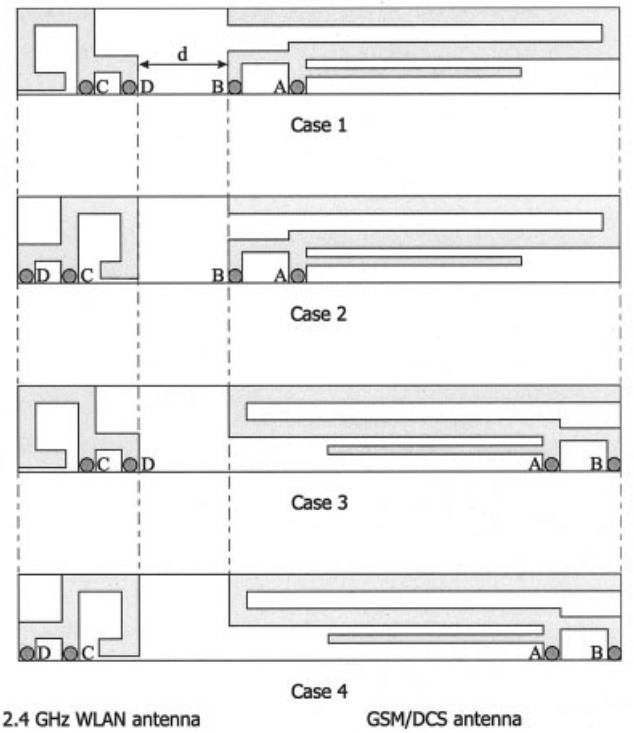

Figure 2 Possible arrangements (cases 1 to 4) of the two integrated GSM/DCS and WLAN antennas. The configuration shown in Fig. 1(a) is for the case 1 arrangement

near the bottom edge of the system circuit board. In this study, the maximum isolation S_{21} values over the GSM, DCS, and WLAN bands are less than -33.6, -27.9, and -33.0 dB, respectively, which are quite good for practical applications [4]. However, in this case, the two antennas need to be separated by a relatively large distance.

In this paper, we present an isolation study that considers two promising internal GSM/DCS and WLAN antennas printed and integrated on a dielectric substrate. In the study, both of the GSM/DCS and WLAN antennas are printed PIFAs of compact size (see Fig. 1) and are suitable to be mounted at the top edge of the system circuit board of a PDA phone as internal antennas. This arrangement provides an alternative antenna design for dual-network wireless devices, in addition to the use of the two separate antennas studied in [4]. The results indicate that by arranging the two integrated antennas back to back (with their shorting strips facing each other), good isolation behavior with S_{21} less than -20 dB over the GSM, DCS, and WLAN bands is achievable. Such an isolation behavior is usually acceptable for most practical applications. Details of the experimental and simulation results are presented and analyzed.

2. TWO INTEGRATED INTERNAL GSM/DCS AND WLAN ANTENNAS

Figure 1(a) shows the configuration of two integrated internal GSM/DCS and WLAN antennas for a dual-network PDA phone. In the figure, the grounded FR4 substrate of dimensions 100×70 mm^2 is treated as the main circuit board of a PDA phone. Both antennas are printed on a 0.8-mm-thick FR4 substrate of narrow width (10 mm), and are in the form of a PIFA with a folded radiating arm in order to achieve a compact size [5]. Detailed dimensions of the two antennas are given in Figures 1(b) and 1(c). Note that the two antennas are spaced with a distance of d, and there are four possible arrangements (denoted as cases 1 to 4 here) of the two antennas (see Fig. 2), and the configuration shown in Figure 1(a) is for the case 1 arrangement. The isolation behavior of the two antennas with the arrangements of cases 1 to 4 is studied first. The optimal arrangement for achieving optimized isolation between the two antennas will be identified. Then, effects of the distance d on the isolation between the two antennas will be analyzed with the aid of Figures 3–5 in section 3.

Also note that the two integrated antennas are mounted perpendicularly at the top edge of a system circuit board [6–8] that shows a low profile of only 10 mm, which makes it very promising to be concealed within the casing of the PDA phone. In addition, for the GSM/DCS antenna, it can generate two operating bands at

TABLE 1 Measured Maximum Isolation (S_{21}) Over the GSM, DCS, and WLAN Bands for Different Arrangements (Cases 1 to 4 Shown in Fig. 2) of the Two Integrated GSM/DCS and WLAN Antennas with d = 11 mm

	Max. S_{21} [dB] In the GSM Band	Max. S_{21} [dB] In the DCS Band	Max. S_{21} [dB] In the WLAN Band
Case 1	−28.5	−20.8	−25.1
Case 2	−25.8	−16.4	−21.5
Case 3	−27.7	−16.7	−21.3
Case 4	−22.7	−11.1	−13.5

Note that for each case the impedance bandwidths of the two antennas are adjusted to cover the operating bands of the GSM, DCS, and WLAN bands.

about 900 and 1800 MHz in order to cover the GSM (890–960 MHz) and DCS (1710–1880 MHz) bands. For the GSM band, it is mainly contributed from the fundamental resonant mode of arm 1. As for the DCS band, it is formed by two resonant modes, one contributed from the second resonant modes of arm 1 and the other from the fundamental mode of arm 2.

For the WLAN antenna, it can generate a wide operating band to cover the 2.4-GHz band (2400–2484 MHz). Note that at the end of the radiating arm [see Fig. 1(c)], there is a tuning length of t for tuning the antenna's resonant frequency to be at about 2.45 GHz when the distance d between the two antennas is varied. In this case when d is varied (in this study, the GSM/DCS antenna is fixed and flushed to the right top corner of the main circuit board [see Fig. 1(a)] and the position of the WLAN antenna is varied to result in a variation in d), the WLAN antenna can easily be tuned to cover the 2.4-GHz band by adjusting the length of t (about 2.0 to 5.6 mm in this study). Also note that, largely because the GSM/DCS antenna is fixed, the resonant frequencies of the GSM/DCS antenna are very slightly affected. Thus, no adjustment of the design dimensions shown in Figure 1(b) is required in the study.

3. RESULTS AND DISCUSSION

The two antennas with the four possible arrangements shown in Figure 2 were constructed and studied. Measured maximum isolation (S_{21}) within the GSM, DCS, and WLAN bands for different arrangements of cases 1 to 4 with $d = 11$ mm is listed in Table 1. Note that, for $d = 11$ mm, both of the GSM/DCS and WLAN antennas are, respectively, flushed to the right and left top corners of the main circuit board studied here. The results clearly indicate that the case 1 arrangement shows optimal isolation between the two antennas; in this case, the isolation (S_{21}) is less than -20 dB for all operating frequencies over the GSM, DCS, and WLAN bands. This behavior is probably because the two integrated antennas in case 1 are arranged to be back to back with their shorting strips facing each other, such that better shielding effects between the two antennas are obtained [8, 9].

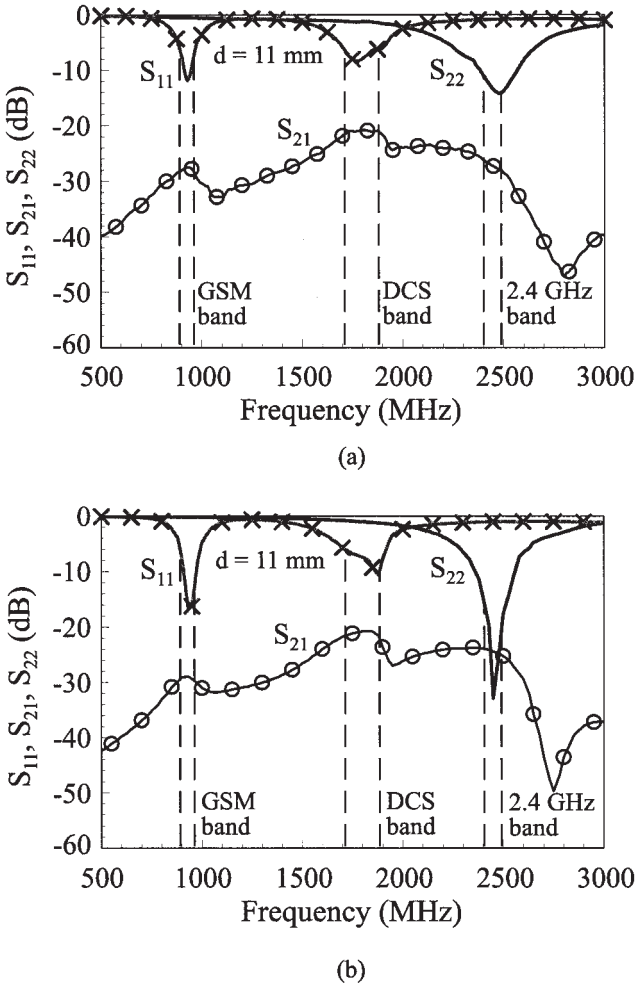

Figure 3 Reflection coefficient (S_{11} for the GSM/DCS antenna, S_{22} for the WLAN antenna) and isolation (S_{21}) between the two antennas for the case 1 arrangement with $d = 11$ mm: (a) measured results; (b) simulated results

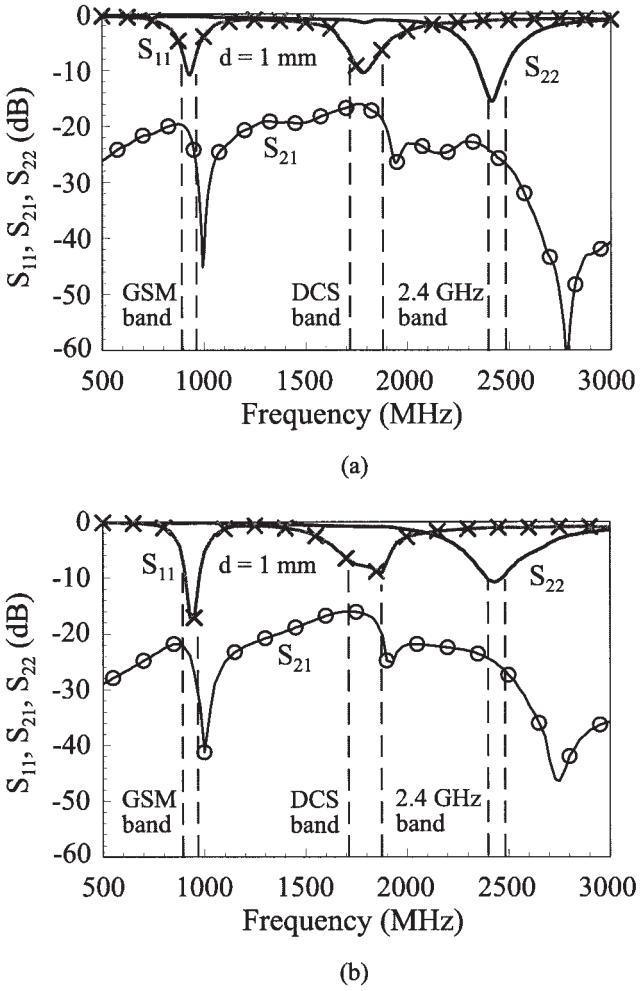

Figure 4 Reflection coefficient (S_{11} for the GSM/DCS antenna, S_{22} for the WLAN antenna) and isolation (S_{21}) between the two antennas for the case 1 arrangement with $d = 1$ mm: (a) measured results; (b) simulated results

The isolation behavior between the two antennas with case 1 arrangement as a function of d is then studied. Figure 3 shows the measured and simulated reflection coefficients (S_{11} for the GSM/DCS antenna, S_{22} for the WLAN antenna) and isolation (S_{21}) between the two antennas with $d = 11$ mm. The corresponding results for $d = 1$ mm are shown in Figure 4. First note that the measured data in general agree with the simulated results obtained using the Ansoft simulation software HFSS (High Frequency Structure Simulator). It is also seen that for either $d = 11$ or 1 mm, the GSM/DCS antenna generates two separate resonant modes at about 900 and 1800 MHz, hence covering the GSM and DCS

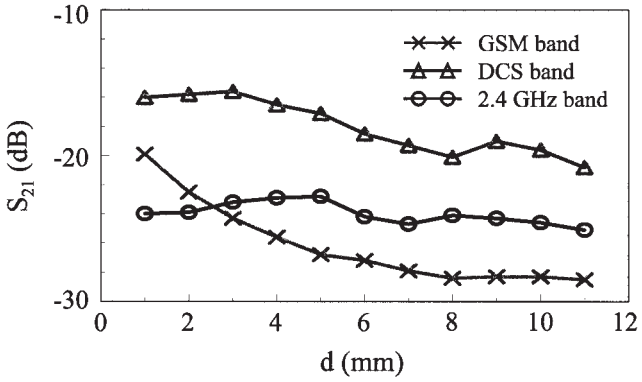

Figure 5 Measured maximum isolation (S_{21}) over the GSM, DCS, and WLAN bands as a function of d for the case 1 arrangement

bands. Similarly, a resonant mode generated by the WLAN antenna also covers the 2.4-GHz band.

For the isolation over the GSM, DCS, and WLAN bands, it is clearly seen that the case with $d = 11$ mm shows better isolation than that with $d = 1$ mm. The measured maximum isolation (S_{21}) over the GSM, DCS, and WLAN bands as a function of d is also presented in Figure 5. Relatively large effects of the distance d on the isolation over the GSM and DCS bands are seen. For the WLAN band, although relatively small effects are observed, the measured isolation is less than -23 dB for all cases. In general, the optimal isolation over the GSM, DCS, and WLAN bands is obtained when $d = 11$ mm. In this case, the measured isolation (S_{21}) over the three operating bands is all less than -20 dB.

4. CONCLUSION

Two integrated internal antennas for GSM/DCS and WLAN operations for a dual-network PDA phone have been presented. An optimized arrangement of the two antennas for achieving optimal isolation has been analyzed. Good isolation between the two antennas with measured maximum isolation (S_{21}) less than -20 dB over the GSM, DCS, and WLAN bands has also been obtained.

REFERENCES

1. A.K. Salkintzis, C. Fors, and R. Pazhyannur, WLAN-GPRS integration for next-generation mobile data networks, IEEE Wireless Commun 9 (2002), 112–124.
2. H. Luo, Z. Jiang, B.J. Kim, N.K. Shankaranarayanan, and P. Henry, Integrating wireless LAN and cellular data for the enterprise, IEEE Internet Computing 7 (2003), 25–33.
3. K.L. Wong, Planar antennas for wireless communications, Wiley, New York, 2003.
4. K.L. Wong, J.H. Chou, S.W. Su, and C.M. Su, Isolation between GSM/DCS and WLAN antennas in a PDA phone, Microwave Opt Technol Lett 45 (2005), 347–352.
5. P.L. Teng, T.W. Chiou, and K.L. Wong, Planar inverted-F antenna with a bent meandered radiation arm for GSM/DCS operation, Microwave Opt Technol Lett 38 (2003), 73–75.
6. P.L. Teng, C.Y. Chiu, and K.L. Wong, Internal planar monopole antenna for GSM/DCS/PCS folder-type mobile phones, Microwave Opt Technol Lett 39 (2003), 106–108.
7. C.Y. Chiu, P.L. Teng, and K.L. Wong, Shorted, folded planar monopole antenna for dual-band mobile phone, Electron Lett 39 (2003), 1301–1302.
8. K.L. Wong, Y.Y. Chen, S.W. Su, and Y.L. Kuo, Diversity dual-band planar inverted-F antenna for WLAN operation, Microwave Opt Technol Lett 38 (2003), 223–225.
9. K.L. Wong, A.C. Chen, and Y.L. Kuo, Diversity metal-plate planar inverted-F antenna for WLAN operation, Electron Lett 39 (2003), 590–591.

EFFICIENT MODELING OF THE TIME-DOMAIN CROSSTALK PHENOMENA IN COUPLED MICROSTRIP LINES

Andrzej S. Ciminski[1] and Bogdan J. Janiczak[2]
[1] Vällingbyvägen
111 1tr, SE 162–63
Vällingby, Sweden
[2] Gdansk University of Technology, Faculty of Electronics
Telecommunications and Informatics
Department of Microwave and Antenna Engineering
Gabriela Narutowicza 11/12
80-952 Gdańsk Wrzeszcz, Poland

Received 24 February 2005

ABSTRACT: *The results of crosstalk modeling in a system of parallel-running coupled microstrip lines terminated with lumped linear loads employing the mixed time/frequency domain approach are presented. While inclusion of the dispersive nature of the microstrip lines results in excellent accuracy between the modeling and measurements, the use of a reliable analytical coupled-line model assures increased efficiency of the numerical processing.* © 2005 Wiley Periodicals, Inc. Microwave Opt Technol Lett 46: 326–331, 2005; Published online in Wiley InterScience (www.interscience.wiley.com). DOI 10.1002/mop.20978

Key words: *coupled microstrip lines; crosstalk; PCB*

1. INTRODUCTION

With the introduction of EMC Directive 89/336/EEC and other compatibility related regulations, the need for proper prediction of prospective electromagnetic hazards that may potentially appear in devices and systems has gained increased importance in the last decade. Although, in the meantime, many efforts have been made toward characterization of various EMC-related physical effects appearing on systems, devices, or printed circuit boards (PCB), there is still a lot of research activity seen in this subject. PCB is considered by many to be the most crucial component of electronic and communication systems nowadays and, as such, responsible to the greatest extent for both system functionality and EMC compliance. One of the major problems appearing within PCB electronic circuitry is the transmission of either analogue signals or (in the majority of contemporary applications) digital signals, leading to reflections, crosstalk, and radiations. Thus, a proper type and geometry of traces [1, 2] in relation to carried signals and a well-designed layout topology can significantly decrease parasitic EMC-related phenomena on circuit boards. Studies of crosstalk as an unwanted coupling between transmission lines and its dependency on so-called logic speed (rise and fall times) have already been documented in the literature [3, 7], including the effect of loss [4] and crosstalk reduction techniques [5]. Unfortunately, the effect of dispersion on crosstalk phenomena has been reported only marginally. The other point is that, despite professional and highly priced specialized EMC-related software, there still exists a gap in the market for handy simulation tools oriented toward medium and small-sized electronic companies.

2. DESCRIPTION OF THE PROBLEM

Crosstalk represents energy coupled from a source trace to a victim trace (Fig. 1) and begins as a driver gate outputs a rising edge to